10-12-2018

Contact Juggling of a Disk With a Disk-Shaped Manipulator

Ji-Chul Ryu

Kevin M. Lynch

Original Citation
J.-C. Ryu and K. M. Lynch, "Contact Juggling of a Disk with a Disk-Shaped Manipulator," IEEE Access, Vol. 6, No. 1, pp. 60286-60293, 2018

IEEE Access
Multidisciplinary | Rapid Review | Open Access Journal

Received September 19, 2018, accepted September 29, 2018, date of publication October 12, 2018,
date of current version November 8, 2018.

Digital Object Identifier 10.1109/ACCESS.2018.2875410

Contact Juggling of a Disk With a Disk-Shaped Manipulator

JI-CHUL RYU[1], (Member, IEEE), AND KEVIN M. LYNCH[2], (Fellow, IEEE)
[1]Mechanical Engineering Department, Northern Illinois University, DeKalb, IL 60115, USA
[2]Neuroscience and Robotics Laboratory and Mechanical Engineering Department, Northwestern University, Evanston, IL 60208, USA

Corresponding author: Ji-Chul Ryu (jryu@niu.edu)

Part of this work was supported by NSF under Grant IIS-0964665.

ABSTRACT In this paper, we present a feedback controller that enables contact juggling manipulation of a disk with a disk-shaped manipulator, called the mobile disk-on-disk. The system consists of two disks in which the upper disk (object) is free to roll on the lower disk (hand) under the influence of gravity. The hand moves with a full three degrees of freedom in a vertical plane. The proposed controller drives the object to follow a desired trajectory through rolling interaction with the hand. Based on the mathematical model of the system, dynamic feedback linearization is used in the design of the controller. The performance of the controller is demonstrated through simulations considering disturbances and uncertainties.

INDEX TERMS Dynamic feedback linearization, nonprehensile manipulation, rolling manipulation, contact juggling.

I. INTRODUCTION

Manipulation is generally about moving an object from one place to another. Methods to manipulate objects broadly fall into two categories: prehensile and nonprehensile. Prehensile manipulation uses grasp restraint characterized by form or force closure at all times. While rigorous definitions are given in [1], roughly speaking the grasp maintains form closure when the object is not allowed to move even infinitesimally. Force closure is achieved when the grasp can be maintained despite any external wrench applied on the restrained object.

For nonprehensile manipulation, the object's motion is achieved by a collaboration between the manipulator controls and dynamics [2], [3]. Examples include rolling, sliding, pushing, throwing, and catching. This type of manipulation allows the generation of complex object motions by a simple low-degree-of-freedom robot. In addition, some tasks, such as throwing and catching, cannot be accomplished by traditional grasping manipulation.

Among the many types of nonprehensile manipulation, one type that we are particularly interested in is contact juggling [4] in which a smooth object, usually a sphere, rolls on another smooth object, e.g., the human hand, arm, head, or body. The generalized problem can then be formulated as follows: *Given a parameterization of the surfaces and the desired trajectory of the object in space, how should the manipulator be controlled to achieve the desired object motion by rolling?*

In this paper, the problem is simplified to a disk-shaped object with a disk-shaped manipulator. This paper builds on our previous work [5] on a rolling manipulation system called the "disk-on-disk" in which feedback stabilization is presented to balance a disk (object) on top of another disk (hand). In addition to balancing, the task of orientation control, i.e., the hand controls the object to a target orientation, or angular velocity control, i.e., the hand spins the object at a target velocity, is achieved simultaneously. In that study, however, the hand only rotates; it cannot translate.

In this paper, we consider the disk-on-disk where the hand moves with a full three degrees of freedom in the plane, as shown in Fig. 1. This offers the possibility to control the full planar trajectory of the object, rather than simply balancing it on top of the hand while achieving orientation or angular velocity control. Our objective in this study is to develop a feedback controller to drive the object along a desired trajectory using rolling manipulation.

We solve this control problem using a similar framework of feedback linearization proposed in the previous study. However, as opposed to the previous system, the mobile disk-on-disk in this work is not statically feedback linearizable. In other words, the nonlinear dynamic equation can only be partially linearized, yielding internal dynamics. Therefore we apply input prolongation. This procedure is called dynamic feedback linearization, which allows the extended system

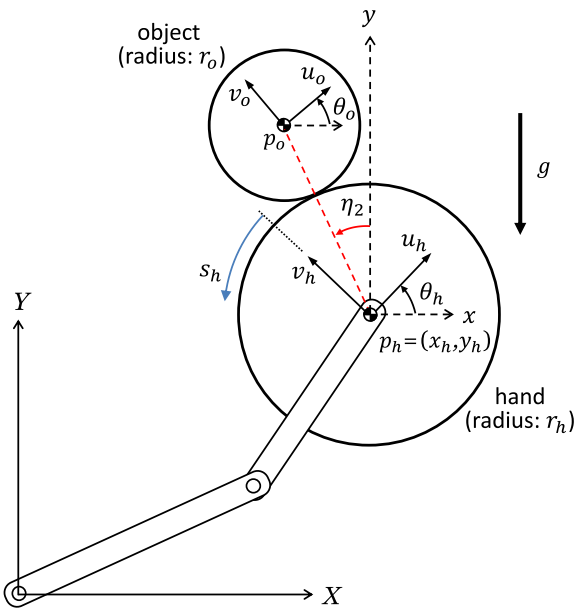

FIGURE 1. Schematic of the mobile disk-on-disk mounted on a two-link arm. The hand can move in a vertical plane under the influence of gravity. The angle η_2 of the object is measured counter-clockwise from the y-axis of the frame attached to the hand center. The x-y coordinate frame only translates with respect to the world X-Y frame.

to become statically feedback linearizable with no internal dynamics [6].

A. RELATED WORK

In the context of contact juggling tricks, the "butterfly" system has been first studied in [7], where the analysis of the shape design of a manipulator in creating rolling motion of an object is presented. An energy-based control technique through swing-up and balancing phases is used to stabilize the butterfly system in [8]. Feasible trajectory planning and feedback control design that ensure stability in a neighborhood of the planned trajectory are presented in [9]. The shape design problem is formulated as a nonlinear optimization problem with the kinematic and dynamic relationships as constraints in [10]. Conditions on the shape of the object and manipulator are identified for a planar rolling manipulation system to be input-state linearizable [11].

Control of rolling manipulation has also been studied in various types of systems including the ball-on-beam. Based on its simplified dynamic model, an approximate input-output linearization method is used to achieve stabilization in [12]. A formulation called interconnection and damping assignment, based on passivity-based control, to stabilize the system is proposed in [13]. This work can be applied to a large class of underactuated systems although it requires kinetic and potential energy shaping. A semi-global stabilization is achieved using a nested saturation-based output feedback controller in [14]. Building on this work, global asymptotic stability is developed in [15] with a saturation control method using state-dependent saturation levels. Sliding mode control for simplified and complete models is studied in [16].

An extension of the ball-on-beam is the ball-on-plate. Following the pioneering work by Montana [17] on kinematics of objects with rolling contact, conditions are given in [18] under which an admissible path exists between two configurations of an object. It is also shown that the motion planning problem can be solved when a path exists. A similar motion planning problem for the ball-on-plate is considered in [19]. The problem becomes more difficult when the sphere has a limited contact area [20]. Controllers for this type of system have been developed based on a discontinuous control strategy for exponential stabilization [21] and non-smooth switching control utilizing the concept of "switching-driving Lyapunov function" [22]. An iterative feedback control based on a nilpotent approximation to the rolling model is presented in [23]. It is shown in [24] that open-loop control is also possible within a small neighborhood of goal orientations despite a bounded perturbation in the ball radius. Typical approaches to the stabilization control problem of the ball-on-plate system use approximate linearization to easily apply linear control techniques. Under a double-loop control structure, a linear state-feedback controller is used in [25]. Approximate input-output feedback linearization is applied in [26]. An I-PD controller, a variant of the PID controller, is proposed to solve the stabilization problem in [27].

The disk-on-disk system that was first studied in [5] can be considered a challenging variant of the ball-on-beam system where the beam is replaced by a disk. While feedback stabilization control is presented in [5], the backstepping method [28] and a passivity-based control [29] are also shown to perform the balancing task. This type of rolling contact manipulation is also important in dexterous grasping as it often appears between fingers and an object [30], [31].

This paper extends our preliminary work in [32] where the hand's position, not the object's, is controlled with no trajectory tracking capability. In this paper, we directly tackle the object position which is more desirable from a manipulation point of view. As a result, this approach enables object trajectory tracking. The stabilization of the object orientation to a target is achieved by stabilizing the hand orientation to the corresponding target. As is the case in [5], the object's angular velocity control while balancing the object on top of the hand can also be performed as a second task.

II. DERIVATION OF THE DYNAMIC MODEL

In this section, we derive the equations of motion of the mobile disk-on-disk system using Lagrange's equation.

A. MOBILE DISK-ON-DISK SYSTEM

The schematic of the mobile disk-on-disk system is shown in Fig. 1 as it is mounted on a (two-link) manipulator arm. The local coordinate frames u_h-v_h and u_o-v_o are attached to the centers of the hand and the object, respectively. The origin of each frame, or the center of each disk, are given by $p_h = [x_h, y_h]^T$ and $p_o = [x_o, y_o]^T$, respectively.

While the detailed geometric background for general planar rolling is available in [5], we only present essential kinematics of the disk-shaped object here that are necessary to derive the dynamic equation.

$$p_o = p_h + \begin{bmatrix} -(r_h + r_o)\sin(\theta_h + s_h/r_h) \\ (r_h + r_o)\cos(\theta_h + s_h/r_h) \end{bmatrix} \tag{1}$$

$$\theta_o = \theta_h + \kappa_r s_h \tag{2}$$

$$\kappa_r = \frac{1}{r_h} + \frac{1}{r_o}. \tag{3}$$

Here, $s_h \in \mathbb{R}$ represents the arclength parameter that parametrizes the curve of the hand, with which the contact point is given by $[-r_h \sin(s_h/r_h), r_h \cos(s_h/r_h)]^T$ in the u_h-v_h frame. κ_r denotes the relative curvature. Notice that the angle represented by $\theta_h + s_h/r_h$ in (1) is the angle of the center of the object measured with respect to the vertical line, described by η_2 in Fig. 1, which will be later driven to zero for stabilization.

B. DYNAMIC EQUATIONS

For simplicity, we initially treat the hand disk as a free-flying body actuated by the linear force (F_x, F_y) and the torque τ_h through and about the center of mass, respectively. Later in this section we simplify further, assuming that the control inputs are the linear acceleration of the object and the angular acceleration of the hand. Transformations between these controls and typical joint torque controls of a robot arm can be accomplished by standard techniques in robotics (e.g., [33] and references therein).

We now derive the equations of motion in terms of the generalized coordinates $q = [x_o, y_o, \theta_h, s_h]^T$ with three inputs: two forces F_x, F_y in the direction of the X and Y axes and torque τ_h about the center of the hand. We use Lagrange's equation,

$$\frac{d}{dt}\frac{\partial L}{\partial \dot{q}} - \frac{\partial L}{\partial q} = Q, \tag{4}$$

where L denotes the Lagrangian $L = K - U$ with the kinetic energy K and potential energy U. The system's K and U are computed as

$$K = \frac{1}{2}\left(m_h \dot{p}_h^T \dot{p}_h + I_h \dot{\theta}_h^2 + m_o \dot{p}_o^T \dot{p}_o + I_o \dot{\theta}_o^2\right) \tag{5a}$$

$$U = g(m_h p_h^T + m_o p_o^T)\begin{bmatrix} 0 \\ 1 \end{bmatrix} \tag{5b}$$

where m_h, I_h and m_o, I_o are the mass and moment of inertia of the hand and object, respectively, and g is the gravitational acceleration.

Substituting p_h from (1) and θ_o from (2) into (5), the dynamic model is subsequently obtained as

$$M(q)\ddot{q} + V(q, \dot{q}) = Q \tag{6}$$

where $Q = [F_x, F_y, \tau_h, 0]^T$. The detailed expressions for $M(q)$ and $V(q, \dot{q})$ are provided in Appendix A. As we mentioned before, we consider the linear accelerations of the object and the angular acceleration of the hand as the inputs to the system such that $[v_x, v_y, v_z]^T = [\ddot{x}_o, \ddot{y}_o, \ddot{\theta}_h]^T$. Rearranging (6) by substituting $\ddot{s}_h$ from the fourth equation into the first three, the input transformation between the forces and accelerations is given by

$$\begin{bmatrix} F_x \\ F_y \\ \tau_h \end{bmatrix} = \begin{bmatrix} a_{11} & a_{12} & a_{13} \\ a_{21} & a_{22} & a_{23} \\ a_{31} & a_{32} & a_{33} \end{bmatrix} \begin{bmatrix} v_x \\ v_y \\ v_z \end{bmatrix} + \begin{bmatrix} b_1 \\ b_2 \\ b_3 \end{bmatrix} \tag{7}$$

where

$$a_{ij} = m_{ij} - m_{i4}m_{4j}/m_{44}$$
$$b_i = V_i - m_{i4}V_4/m_{44}.$$

See Appendix A for m_{ij} and V_i. It should be mentioned that θ_o cannot be selected as a generalized coordinate together with x_o and y_o since in that case the transformation (7) cannot be constructed due to the lack of the $\ddot{s}_h$ term in the fourth equation of motion in (6). However, the control of the object orientation θ_o at stabilization can still be achieved through θ_h, which is explained in Section IV-A.

III. DYNAMIC FEEDBACK LINEARIZATION CONTROL

In this section, we show how to design a feedback controller using dynamic feedback linearization through a change of coordinates and input prolongation. As a result, the system will be equivalently characterized by three decoupled linear integrators.

A. INPUT PROLONGATION WITH CHANGE OF COORDINATES

The equations of motion in (6) can be rewritten in state-space representation in terms of 8-dimensional state variables $z = [x_o, \dot{x}_o, y_o, \dot{y}_o, \theta_h, \dot{\theta}_h, s_h, \dot{s}_h]^T$ with acceleration inputs v_x, v_y, and v_z.

$$\begin{aligned} \dot{z}_1 &= z_2 \\ \dot{z}_2 &= v_x \\ \dot{z}_3 &= z_4 \\ \dot{z}_4 &= v_y \\ \dot{z}_5 &= z_6 \\ \dot{z}_6 &= v_z \\ \dot{z}_7 &= z_8 \\ \dot{z}_8 &= -\frac{1}{m_{44}}\left(m_{41}v_x + m_{42}v_y + m_{43}v_z + V_4\right) \end{aligned} \tag{8}$$

It can be checked that the system above is not statically feedback linearizable [6, Ch. 12]. In other words, when an input-output linearization is conducted, internal dynamics will appear. Therefore, we introduce two input prolongations for each of v_x and v_y, along with the following change of coordinates

$$\eta_1 = m_{43}\dot{\theta}_h + m_{44}\dot{s}_h \tag{9a}$$

$$\eta_2 = \theta_h + s_h/r_h \tag{9b}$$

$$\delta = \theta_h - \theta_h^* \tag{9c}$$

$$\xi = \dot{\theta}_h \tag{9d}$$

where m_{43} and m_{44} are the constant elements of $M(q)$ in (6) and the expressions are provided in (29) in Appendix A. θ_h^* is the target orientation of the hand corresponding to that of the object. By the input prolongations, four additional state variables of v_x, u_x, v_y, and u_y are employed. Then, the prolonged dynamic model is expressed as

$$\begin{aligned}
\dot{z}_1 &= z_2 \\
\dot{z}_2 &= v_x \\
\dot{v}_x &= u_x \\
\dot{u}_x &= \omega_x \\
\dot{z}_3 &= z_4 \\
\dot{z}_4 &= v_y \\
\dot{v}_y &= u_y \\
\dot{u}_y &= \omega_y \\
\dot{\eta}_1 &= (\alpha_1 \cos\eta_2)v_x + (\alpha_1 \sin\eta_2)v_y + \alpha_1 g \sin\eta_2 \\
\dot{\eta}_2 &= \alpha_2\eta_1 + \alpha_3\xi \\
\dot{\delta} &= \xi \\
\dot{\xi} &= v_z
\end{aligned} \tag{10}$$

where $\alpha_1 \equiv m_o r_o \kappa_r$, $\alpha_2 \equiv 1/(r_h I_o \kappa_r^2)$, and $\alpha_3 \equiv 1/(r_o\kappa_r)$. Now, ω_x and ω_y are new inputs to the system along with the original input v_z. Note that the original inputs v_x and v_y and their first derivatives are now considered state variables.

B. FEEDBACK LINEARIZATION

It can be proven that the prolonged system in (10) is now statically feedback linearizable with the three linearizing outputs chosen as $h_1 = x_o$, $h_2 = y_o$, and $h_3 = \eta_2 - \alpha_3\delta$. Taking derivatives of these three outputs until an input appears yields

$$h_1^{(4)} = \omega_x \tag{11}$$
$$h_2^{(4)} = \omega_y \tag{12}$$
$$\dot{h}_3 = \dot{\eta}_2 - \alpha_3\dot{\delta} = \alpha_2\eta_1 \tag{13}$$
$$\ddot{h}_3 = \alpha_2\alpha_1 v_x c_2 + \alpha_2\alpha_1 v_y s_2 + \alpha_2\alpha_1 g s_2 \tag{14}$$
$$\begin{aligned}\dddot{h}_3 &= \alpha_2\alpha_1(\alpha_2\eta_1 + \alpha_3\xi)(-v_x s_2 + v_y c_2 + g c_2) \\ &\quad + \alpha_2\alpha_1(u_x c_2 + u_y s_2)\end{aligned} \tag{15}$$
$$h_3^{(4)} = \beta(x) + \gamma_1(x)\omega_x + \gamma_2(x)\omega_y + \gamma_3(x)v_z \tag{16}$$

where s_2 and c_2 denote $\sin\eta_2$ and $\cos\eta_2$, respectively and

$$\gamma_1(x) = \alpha_2\alpha_1 \cos\eta_2 \tag{17}$$
$$\gamma_2(x) = \alpha_2\alpha_1 \sin\eta_2 \tag{18}$$
$$\gamma_3(x) = \alpha_2\alpha_1\alpha_3(-v_x \sin\eta_2 + v_y \cos\eta_2 + g\cos\eta_2) \tag{19}$$

with 12-dimensional $x = [z_{1-4}, v_x, u_x, v_y, u_y, \eta_1, \eta_2, \delta, \xi]^T$. Due to its length, the detailed expression for $\beta(x)$ is provided in Appendix A.

As shown in (11), (12), and (16), the total relative degree of the prolonged system is 12 which is equal to the dimension of the prolonged system in (10). This ensures that the system is now statically feedback linearizable yielding no internal dynamics.

Finally, we obtain decoupled quadruple linear integrators.

$$h_1^{(4)} = \chi_1 \tag{20a}$$
$$h_2^{(4)} = \chi_2 \tag{20b}$$
$$h_3^{(4)} = \chi_3 \tag{20c}$$

with the input transformation

$$\begin{bmatrix}\omega_x \\ \omega_y \\ v_z\end{bmatrix} = \Gamma^{-1}\left(\begin{bmatrix}\chi_1 \\ \chi_2 \\ \chi_3\end{bmatrix} - \begin{bmatrix}0 \\ 0 \\ \beta(x)\end{bmatrix}\right) \tag{21}$$

where

$$\Gamma = \begin{bmatrix}1 & 0 & 0 \\ 0 & 1 & 0 \\ \gamma_1 & \gamma_2 & \gamma_3\end{bmatrix}.$$

Note that this feedback linearization is not an approximation. The system described by (20) is exactly equivalent to the original system (6). It should also be pointed out that this input transformation has a singularity where $\gamma_3 = 0$ in which Γ^{-1} does not exist. The singular point is determined by η_2 configuration and accelerations $(\ddot{x}_o, \ddot{y}_o)$ of the object as seen in (19). This is the case when the normal force between the hand and the object is zero, so the object becomes uncontrollable due to loss of contact.

For these decoupled quadruple integrators, the control law can be designed as

$$\chi_i = h_i^{d(4)} + K_i y_i \tag{22}$$

where $y_i = [h_i^d - h_i, \dot{h}_i^d - \dot{h}_i, \ddot{h}_i^d - \ddot{h}_i, \dddot{h}_i^d - \dddot{h}_i]^T$ and h_i^d is a differentiable desired trajectory of at least class C^4. K_i is a row gain matrix. This control law makes the error dynamics converge to zero with control gains chosen to have a Hurwitz matrix.

IV. SIMULATION RESULTS

In this section, we present simulation results to demonstrate the proposed dynamic feedback linearization controller. As the object is controlled to follow a desired trajectory, the object is also driven to the upright position as well as the target orientation simultaneously. As the stability and convergence of the system is guaranteed theoretically with the linear controller in (22) for the transformed linear system in (20), in order to evaluate the performance of the proposed controller in a more realistic fashion, we considered disturbance, noise, and uncertainty in the simulations. Since disturbances to the system can be considered as an additional input, we added 20% of the weight of the object each to the calculated input χ_1 and χ_2. Also 20% of the weight of the hand was added to χ_3 in (22). In addition, an added 5% of the actual value was considered in the feedback of the state variables in the calculation of the control inputs in (22), which would basically account for measurement noise as well as parameter uncertainty. All units are SI unless otherwise noted.

A. TRAJECTORY TRACKING WITH BALANCING

In this simulation, for simplicity a time-parameterized polynomial of degree 5 is used for each desired trajectory of $x^d(t)$ and $y^d(t)$ so that its coefficients can be uniquely determined by its initial and final conditions. With a chosen travel time of $t_f = 5$ sec, the following end conditions are used:

$$\begin{aligned} x^d(0) &= -0.5, \quad \dot{x}^d(0) = 0, \ \ddot{x}^d(0) = 0 \\ x^d(t_f) &= 0, \quad \dot{x}^d(t_f) = 0, \ \dot{x}^d(t_f) = 0 \\ y^d(0) &= -0.5, \quad \dot{y}^d(0) = 0.1, \ \ddot{y}^d(0) = 0 \\ y^d(t_f) &= 0, \quad \dot{y}^d(t_f) = 0.1, \ \ddot{y}^d(t_f) = 0 \end{aligned}$$

The given initial conditions are $(x_o(0), y_o(0), \theta_h(0), \eta_2(0)) = (-0.45, -0.5, 0, \frac{\pi}{7})$ and the disks start from rest yielding zero initial conditions for all the other variables. To show the trajectory tracking capability, an error of 0.05 is set to the initial x_o position and an error of 0.1 to the initial $\dot{y}_o$, in addition to the disturbances and uncertainties added to the simulation, as shown in Fig. 3.

For the desired trajectory of the output h_3, we use $h_3^d(t) = 0$ only to stabilize it to the origin since trajectory tracking of h_3 has no physical meaning. The gains of $K_i = [81\ 108\ 54\ 12]$ are selected for all three χ_i in (22), which correspond to having repeated poles at -3 in the s-plane.

The target orientation of the object is chosen as $\theta_o^* = \frac{\pi}{2}$. Since this object's target orientation is achieved by controlling the hand orientation, we use the following relationship which is valid in steady state.

$$\theta_h^* = -\frac{r_o}{r_h}\theta_o^* \tag{23}$$

which can be derived from (2) and (9b) when $\eta_2 = 0$.

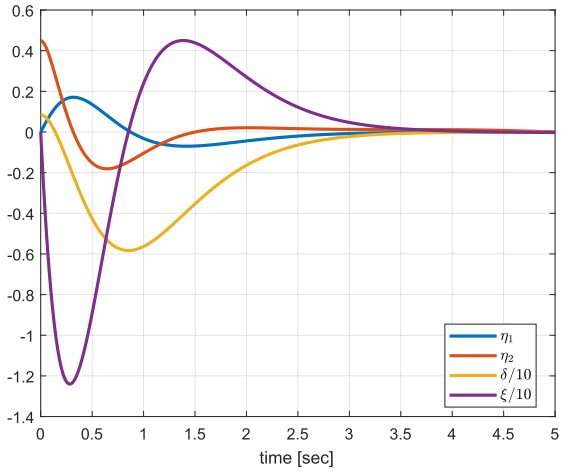

FIGURE 2. Simulation results. The quantities $\frac{1}{10}\delta$ and $\frac{1}{10}\xi$ are plotted here to be shown on the same scale of other variables. The convergence of the state variables to zero indicates that the object becomes balanced at the upright position and the target orientation.

As Fig. 2 shows, the state variables almost converge to the origin despite the disturbances. Although the effect of the disturbances is clearer in Fig. 3, the system still shows it is capable of tracking the desired trajectory while correcting the initial error.

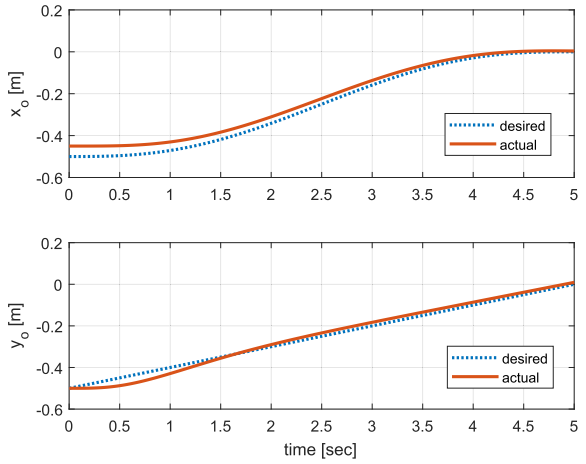

FIGURE 3. Desired and actual trajectories of the object position. An initial error of 0.05 m is given in x_o and the system starts from rest whereas the desired initial y-velocity is chosen as 0.1 m/s.

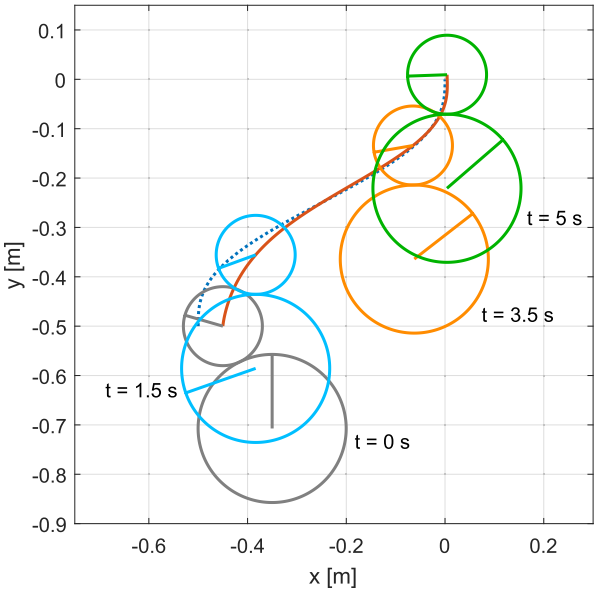

FIGURE 4. Snapshots that show the position and configuration of the disks at $t = 0$, 1.5, 3.5, and 5 seconds, respectively. The dotted line is the desired trajectory and the solid line represents the actual object trajectory.

Fig. 4 shows the configuration of the disks at four times during the manipulation. Initially the object is positioned at an angle of $\eta_2(0) = \frac{\pi}{7}$ (25.7 deg) with respect to the y-axis. It is observed that the object is stabilized to 92.0 deg under the disturbances while the target orientation is $\theta_o^* = 90.0$ deg. In addition, the object is balanced at the upright position at $t = t_f$ with an error of only 0.05 deg for η_2. The desired and actual trajectories of the object are plotted in a dotted and a solid line, respectively.

B. NORMAL FORCE AND FRICTION COEFFICIENT

The dynamic model derived in previous sections always assumes rolling contact. That is, for some states and controls a negative normal force may be required, which implies losing contact in reality. The normal force N must be always positive

to ensure that the hand "holds" the object at all times. In addition, in order for the disks not to slip, the magnitude of the friction force F_t must be equal to or less than the maximum static friction. These conditions are expressed as

$$N > 0 \tag{24}$$
$$|F_t| \leq \mu N. \tag{25}$$

Using a free-body diagram of the object, the normal and friction forces can be determined in terms of the angle η_2 and the accelerations of the object.

$$N = m_o(v_y + g)\cos\eta_2 - m_o v_x \sin\eta_2 \tag{26}$$
$$F_t = m_o(v_y + g)\sin\eta_2 + m_o v_x \cos\eta_2. \tag{27}$$

Fig. 5 shows the calculated normal force and required minimum friction coefficient during the simulated motion. It shows the normal force is always positive ensuring contact during the motion.

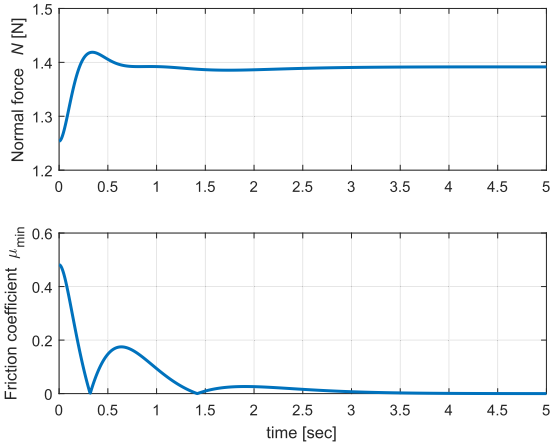

FIGURE 5. The normal force and required minimum friction coefficient during the simulated manipulation. The positive normal force at all times ensures no loss of contact.

C. BALANCING WITH A CONSTANT ANGULAR VELOCITY

As is the case in [5], the task of balancing with a constant angular velocity can also be conducted under the same framework with a slight modification of $\delta = \theta_h - \dot{\theta}_h^* t$ in (9c). Here, t is time and $\dot{\theta}_h^*$ is the target hand angular velocity. With the same linearizing output $h_3 = \eta_2 - \alpha_3\delta$, the first derivative $\dot{h}_3$ in (13) now turns out to be $\dot{h}_3 = \alpha_2\eta_1 + \alpha_3\dot{\theta}_h^*$. However, since $\dot{\theta}_h^*$ is constant, the further derivatives of h_3 do not change. Therefore, the same control law given in (22) can still be used for this velocity control task. The target angular velocity of the object can be similarly set through that of the hand.

$$\dot{\theta}_h^* = -\frac{r_o}{r_h}\dot{\theta}_o^* \tag{28}$$

Fig. 6 shows the simulation result under the same amount of the disturbances and uncertainties, used in Section IV-A, for $\dot{\theta}_o^* = 8$ rad/s, which is equivalently $\dot{\theta}_h^* = -4.27$ rad/s with $r_h = 0.15$ and $r_o = 0.08$. The same initial conditions and control gains from Section IV-A are used. As shown in

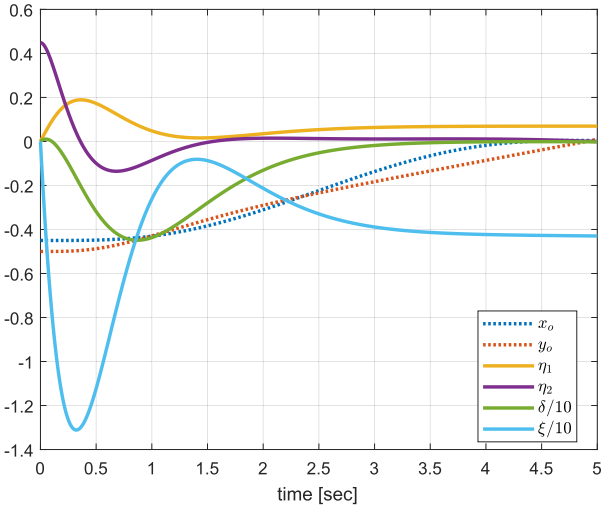

FIGURE 6. The balancing simulation results with velocity control. The plot shows the hand velocity ξ converges to the target velocity of -4.30 rad/s under the disturbances while the target value was -4.27 rad/s.

the figure, the hand angular velocity ξ converges to -4.30 rad/s yielding the object velocity of 8.06 rad/s whereas the target object velocity was 8 rad/s.

V. CONCLUSION

The study presented in this paper built on the authors' previous work on rolling manipulation of the disk-on-disk. The system is enhanced in a way that it is attached to a manipulator arm so that the lower disk moves in translation as well as rotation to perform contact juggling manipulation. However, we did not consider the arm's motion directly in this paper in order to provide more generalized control by assuming we can separately control the force at the arm's end point to which the hand is attached. We designed a controller that enables the object to follow a desired trajectory while stabilizing it to a target orientation as well as balancing it on top of the hand. The full-state, dynamic feedback linearization method is applied along with input prolongations and a change of coordinates. The performance of the controller is demonstrated through simulation results considering disturbances as well as measurement noise and parameter uncertainties. Some potential practical issues would be (i) the desired trajectory needs to be carefully planned so that the manipulated motion can guarantee positive normal force at all times and (ii) the controller requires full state feedback including acceleration and jerk, but the measurement of those quantities may not be easily available.

APPENDIX A

In (6),

$$M(q) = \begin{pmatrix} m_h + m_o & 0 & m_{13} & m_{14} \\ 0 & m_h + m_o & m_{23} & m_{24} \\ m_{31} & m_{32} & m_{33} & m_{34} \\ m_{41} & m_{42} & m_{43} & m_{44} \end{pmatrix} \tag{29}$$

where, with $\eta_2 \equiv \theta_h + \frac{s_h}{r_h}$,

$$
\begin{aligned}
m_{13} &= m_h r_h r_o \kappa_r \cos\eta_2 \\
m_{14} &= m_h r_o \kappa_r \cos\eta_2 \\
m_{23} &= m_h r_h r_o \kappa_r \sin\eta_2 \\
m_{24} &= m_h r_o \kappa_r \sin\eta_2 \\
m_{31} &= -m_o r_h r_o \kappa_r \cos\eta_2 \\
m_{32} &= -m_o r_h r_o \kappa_r \sin\eta_2 \\
m_{33} &= I_o + I_h \\
m_{34} &= I_o \kappa_r \\
m_{41} &= -m_o r_o \kappa_r \cos\eta_2 \\
m_{42} &= -m_o r_o \kappa_r \sin\eta_2 \\
m_{43} &= m_{34} \\
m_{44} &= I_o \kappa_r^2 \\
V(q,\dot{q}) &= \begin{pmatrix} V_1 \\ V_2 \\ V_3 \\ V_4 \end{pmatrix} \\
V_1 &= -m_h(r_h + r_o)\dot{\eta}_2^2 \sin\eta_2 \\
V_2 &= m_h(r_h + r_o)\dot{\eta}_2^2 \cos\eta_2 + (m_h + m_o)g \\
V_3 &= -m_o g(r_h + r_o)\sin\eta_2 \\
V_4 &= -m_o g r_o \kappa_r \sin\eta_2. \qquad (30)
\end{aligned}
$$

In (16),

$$
\begin{aligned}
\beta(x) = &-\alpha_1\alpha_2^2\dot{\eta}_1(v_x \sin\eta_2 - v_y \cos\eta_2 - g\cos\eta_2) \\
&-\alpha_1\alpha_2\dot{\eta}_2^2(v_x \cos\eta_2 + v_y \sin\eta_2 + g\sin\eta_2) \\
&-2\alpha_1\alpha_2\dot{\eta}_2(u_x \sin\eta_2 - u_y \cos\eta_2). \qquad (31)
\end{aligned}
$$

REFERENCES

[1] D. Prattichizzo and J. C. Trinkle, "Grasping," in *Springer Handbook of Robotics*, 2nd ed., B. Siciliano and O. Khatib, Eds. Berlin, Germany: Springer, 2016, ch. 38.

[2] K. M. Lynch and M. T. Mason, "Dynamic nonprehensile manipulation: Controllability, planning, and experiments," *Int. J. Robot. Res.*, vol. 18, no. 1, pp. 64–92, 1999.

[3] K. M. Lynch and T. D. Murphey, "Control of nonprehensile manipulation," in *Control Problems in Robotics*. New York, NY, USA: Springer-Verlag, 2003, pp. 39–57.

[4] J. Ernest, *Contact Juggling*, 3rd ed. Ernest Graphics Press, 2011.

[5] J.-C. Ryu, F. Ruggiero, and K. M. Lynch, "Control of nonprehensile rolling manipulation: Balancing a disk on a disk," *IEEE Trans. Robot.*, vol. 29, no. 5, pp. 1152–1161, Oct. 2013.

[6] H. K. Khalil, *Nonlinear Systems*, 3rd ed. Upper Saddle River, NJ, USA: Prentice-Hall, 2002.

[7] K. M. Lynch, N. Shiroma, H. Arai, and K. Tanie, "The roles of shape and motion in dynamic manipulation: The butterfly example," in *Proc. IEEE Int. Conf. Robot. Autom.*, May 1998, pp. 1958–1963.

[8] M. Cefalo, L. Lanari, and G. Oriolo, "Energy-based control of the butterfly robot," in *Proc. 8th Int. IFAC Symp. Robot Control*, vol. 8, 2006, p. 790.

[9] M. Surov, A. Shiriaev, L. Freidovich, S. Gusev, and L. Paramonov, "Case study in non-prehensile manipulation: Planning and orbital stabilization of one-directional rollings for the 'Butterfly' robot," in *Proc. IEEE Int. Conf. Robot. Autom.*, May 2015, pp. 1484–1489.

[10] O. T. Taylor, "Optimal shape and motion planning for dynamic planar manipulation," M.S. thesis, Dept. Mech. Eng., Massachusetts Inst. Technol., Cambridge, MA, USA, 2017.

[11] V. Lippiello, F. Ruggiero, and B. Siciliano, "The effect of shapes in input-state linearization for stabilization of nonprehensile planar rolling dynamic manipulation," *IEEE Robot. Autom. Lett.*, vol. 1, no. 1, pp. 492–499, Jan. 2016.

[12] J. Hauser, S. Sastry, and P. Kokotovic, "Nonlinear control via approximate input-output linearization: The ball and beam example," *IEEE Trans. Autom. Control*, vol. 37, no. 3, pp. 392–398, Mar. 1992.

[13] R. Ortega, M. W. Spong, F. Gómez-Estern, and G. Blankenstein, "Stabilization of a class of underactuated mechanical systems via interconnection and damping assignment," *IEEE Trans. Autom. Control*, vol. 47, no. 8, pp. 1218–1233, Aug. 2002.

[14] A. R. Teel, "Semi-global stabilization of the 'ball and beam' using 'output' feedback," in *Proc. Amer. Control Conf.*, Jun. 1993, pp. 2577–2581.

[15] C. Barbu, R. Sepulchre, W. Lin, and P. V. Kokotovic, "Global asymptotic stabilization of the ball-and-beam system," in *Proc. 36th IEEE Conf. Decis. Control*, vol. 3, Dec. 1997, pp. 2351–2355.

[16] N. B. Almutairi and M. Zribi, "On the sliding mode control of a ball on a beam system," *Nonlinear Dyn.*, vol. 59, nos. 1–2, pp. 221–238, 2010.

[17] D. J. Montana, "The kinematics of contact and grasp," *Int. J. Robot. Res.*, vol. 7, no. 3, pp. 17–32, 1988.

[18] Z. Li and J. Canny, "Motion of two rigid bodies with rolling constraint," *IEEE Trans. Robot. Autom.*, vol. 6, no. 1, pp. 62–72, May 1990.

[19] R. Mukherjee, M. A. Minor, and J. T. Pukrushpan, "Motion planning for a spherical mobile robot: Revisiting the classical ball-plate problem," *ASME Trans. J. Dyn. Syst., Meas., Control*, vol. 124, no. 4, pp. 502–511, 2002.

[20] M. Svinin and S. Hosoe, "Motion planning algorithms for a rolling sphere with limited contact area," *IEEE Trans. Robot.*, vol. 24, no. 3, pp. 612–625, Jun. 2008.

[21] T. Das and R. Mukherjee, "Exponential stabilization of the rolling sphere," *Automatica*, vol. 40, no. 11, pp. 1877–1889, 2004.

[22] D. Casagrande, A. Astolfi, and T. Parisini, "Switching-driving Lyapunov function and the stabilization of the ball-and-plate system," *IEEE Trans. Autom. Control*, vol. 54, no. 8, pp. 1881–1886, Aug. 2009.

[23] G. Oriolo and M. Vendittelli, "A framework for the stabilization of general nonholonomic systems with an application to the plate-ball mechanism," *IEEE Trans. Robot.*, vol. 21, no. 2, pp. 162–175, Apr. 2005.

[24] A. Becker and T. Bretl, "Approximate steering of a plate-ball system under bounded model perturbation using ensemble control," in *Proc. IEEE/RSJ Int. Conf. Intell. Robots Syst. (IROS)*, Oct. 2012, pp. 5353–5359.

[25] S. Awtar, C. Bernard, N. Boklund, A. Master, D. Ueda, and K. Craig, "Mechatronic design of a ball-on-plate balancing system," *Mechatronics*, vol. 12, no. 2, pp. 217–228, 2002.

[26] M.-T. Ho, Y. Rizal, and L.-M. Chu, "Visual servoing tracking control of a ball and plate system: Design, implementation and experimental validation," *Int. J. Adv. Robot. Syst.*, vol. 10, no. 7, p. 287, 2013.

[27] S. Mochizuki and H. Ichihara, "I-PD controller design based on generalized KYP lemma for ball and plate system," in *Proc. IEEE Eur. Control Conf.*, Jul. 2013, pp. 2855–2860.

[28] J.-C. Ryu, F. Ruggiero, and K. M. Lynch, "Control of nonprehensile rolling manipulation: Balancing a disk on a disk," in *Proc. IEEE Int. Conf. Robot. Autom.*, May 2012, pp. 3232–3237.

[29] A. Donaire, F. Ruggiero, L. R. Buonocore, V. Lippiello, and B. Siciliano, "Passivity-based control for a rolling-balancing system: The nonprehensile disk-on-disk," *IEEE Trans. Control Syst. Technol.*, vol. 25, no. 6, pp. 2135–2142, Nov. 2017.

[30] K. Tahara, S. Arimoto, and M. Yoshida, "Dynamic object manipulation using a virtual frame by a triple soft-fingered robotic hand," in *Proc. IEEE Int. Conf. Robot. Autom.*, May 2010, pp. 4322–4327.

[31] R. R. Ma and A. M. Dollar, "On dexterity and dexterous manipulation," in *Proc. 15th Int. Conf. Adv. Robot.*, Jun. 2011, pp. 1–7.

[32] J.-C. Ryu and K. M. Lynch, "Rolling manipulation control of the disk-on-disk on a two-link arm," in *Proc. IEEE Int. Conf. Mechatron. Automat. (ICMA)*, Aug. 2016, pp. 840–845.

[33] L. Villani and J. De Schutter, "Force control," in *Springer Handbook of Robotics*, 2nd ed., B. Siciliano and O. Khatib, Eds. Berlin, Germany: Springer, 2016, ch. 9.

JI-CHUL RYU received the B.S. and M.S. degrees in mechanical engineering from Korea Advanced Institute of Science and Technology and the Ph.D. degree in mechanical engineering from the University of Delaware in 2009. He is currently an Assistant Professor with the Department of Mechanical Engineering, Northern Illinois University. His research interests include integrated planning and control of autonomous robotic systems, its application to mobility assistive robots, robotic dynamic manipulations, and human-robot interaction for collaboration. He is a member of ASME, affiliated with Dynamic Systems & Control and IEEE, affiliated with the Robotics and Automation Society. He is also a member of editorial board of international research journals, including *Frontiers in Robotics and AI* and *Advances in Robotics Research*.

KEVIN M. LYNCH received the B.S.E. degree in electrical engineering from Princeton University, Princeton, NJ, USA, in 1989, and the Ph.D. degree in robotics from Carnegie Mellon University, Pittsburgh, PA, USA, in 1996. He is currently a Professor and the Chair of the Mechanical Engineering Department, Northwestern University, Evanston, IL, USA. He is also a member of the Neuroscience and Robotics Laboratory and the Northwestern Institute on Complex Systems. He has co-authored *Principles of Robot Motion* (MIT Press, 2005), *Embedded Computing and Mechatronics* (Elsevier, 2015), and *Modern Robotics: Mechanics, Planning, and Control* (Cambridge University Press, 2017). His research interests include dynamics, motion planning, and control for robot manipulation and locomotion, self-organizing multiagent systems, and functional electrical stimulation for restoration of human function. He is Editor-in-Chief of the IEEE TRANSACTIONS ON ROBOTICS.